# Evaluation of chemical composition and physical properties of bituminous binders and fractions

Apostolidis, Panos; Porot, Laurent

**DOI**
10.1080/14680629.2023.2194428

**Publication date**
2023

**Document Version**
Final published version

**Published in**
Road Materials and Pavement Design

Road Materials and Pavement Design

ISSN: (Print) (Online) Journal homepage: https://www.tandfonline.com/loi/trmp20

# Evaluation of chemical composition and physical properties of bituminous binders and fractions

Panos Apostolidis & Laurent Porot

**To cite this article:** Panos Apostolidis & Laurent Porot (08 Jan 2024): Evaluation of chemical composition and physical properties of bituminous binders and fractions, Road Materials and Pavement Design, DOI: 10.1080/14680629.2023.2194428

**To link to this article:** https://doi.org/10.1080/14680629.2023.2194428

ROAD MATERIALS AND PAVEMENT DESIGN
https://doi.org/10.1080/14680629.2023.2194428

Taylor & Francis
Taylor & Francis Group



# Evaluation of chemical composition and physical properties of bituminous binders and fractions

Panos Apostolidis [a] and Laurent Porot [b]

[a]Section of Pavement Engineering, Faculty of Civil Engineering and Sciences, Delft University of Technology, Delft, the Netherlands; [b]Kraton Polymers B.V., Almere, the Netherlands

**ABSTRACT**

Bituminous binders are foreseen as colloidal dispersed systems characterised by high chemical complexity containing a plethora of molecules classified into maltenes and asphaltenes. The effect of these fractions on the overall response of bituminous binders remains elusive. This research selected two binders from the same refinery but with different paving grades. First, Dynamic Shear and Bending Beam Rheometers were employed to assess their rheological properties, and results were consistent with the physical measurements conducted on binders to address low to high temperature rheological response. Then, the binders and their fractions were individually analysed in a Fourier transform infrared spectroscopy and differential scanning calorimetry to elucidate their chemistry associated with the structural changes. No significant difference could be noticed in the infrared spectra of binders, even if they displayed diverse physical properties. Differences may be identified in asphaltenes, an observation which is also supported by calorimetric measurements where steric hindrance occurred upon heating. Maltenes contributed significantly to the glass transition of both binders, while the impact of asphaltenes on the heat capacity changes in glass transition was limited. The findings from this research could be used to establish a new analytical approach for bituminous binders to understand the differences in the physical properties of binders based on their chemistry.

**ARTICLE HISTORY**
Received 1 December 2022
Accepted 19 March 2023

**KEYWORDS**
bitumen; binder; asphalt; dynamic shear rheometer; Fourier transform infrared; differential scanning calorimetry

## Introduction

The advent of polymers and liquid additives as modification technologies and the comprehensive research to understand the chemistry and morphology of bituminous binders have been among the critical advances in pavement engineering of the past decades (Adams et al., 2019; Lesueur, 2009). Recent studies have contemplated making specific changes to the endogenous species and fractions of binders to enable targeted alterations on their colloidal structure. The bituminous binders are foreseen as colloidal dispersed systems characterised by high chemical complexity containing a plethora of molecules, classified based on their differences in polarity and solubility into maltenes and asphaltenes (Corbett, 1969; NASEM, 2017). The asphaltenes contain the heaviest poly-condensed naphtheno-aromatic substances associated mainly with heteroatoms (i.e. O, S and N) in the cycles or peripheral substituents with molecular weight from 1000 to 100,000 Da. It is believed that these substances are responsible for the formation of supramolecular structures of high practical potential, such

**CONTACT** Panos Apostolidis P.Apostolidis@tudelft.nl

as hybrid nanomaterials (Kamkar & Natale, 2021; Schuler et al., 2020). Maltenes are sub-divided in saturates, aromatics, and resin groups based on their polarity and form the medium where asphaltenes are dispersed. Saturates are straight and branch aliphatic chains having small aromatic rings, non-polar and viscous like oil, including wax and non-waxy saturates. The aromatics are molecular compounds in the range of 300–2000 Da and are present in a larger proportion. The resins are solid or semi-solid polar and strongly adhesive with molecular weight between 500 and 50,000 Da (Hunter et al., 2015). Nevertheless, an in-depth understanding of the effect of individual fractions on the thermal properties associated with the structural changes of bituminous binders remains elusive.

The phase morphology of bituminous binders is determined by the structural transitions between the various substances under different conditions. These transitions are grouped into structural and relaxation. On the one hand, the structural changes, over temperature, from less ordering to more ordering conditions are recognised as a phase transition. On the other hand, the relaxation transition reflects the material state through relaxation time and external action. Both formation mechanisms of colloidal dispersion structures of binders can be identified by conducting studies in differential scanning calorimetry (DSC). Especially, the glass transition temperature, which is the temperature that corresponds to the transition region from an amorphous to a glassy state, and the melting point temperature of asphaltenes, derived from vacuum residues, have been determined as 294°C and 452°C, respectively (Kopsch, 1994). Interestingly, other studies in asphaltenes of different geological origins have displayed different DSC thermographs reporting different glass transitions (Evdokimov & Losev, 2010; Masson et al., 2002; Yasar et al., 2007; Zhang et al., 2004). Energy changes of various intensities are also observed in the heat flow curves of asphaltenes and the corresponding bituminous binders. According to Masson et al. (2005), the energy changes of the asphaltenes upon heating are dependent on the annealing time, reflecting the isotropization of ordered amorphous components in these substances. It was reported in the same study that the isotropization of the asphaltenic mesophase, or the segregation of asphaltenes in the maltenic phase, occurs at 40–50°C, and the steric hindrance below 60°C. Nevertheless, the steric hindrance, a consequence of steric effects arising when atoms come close together, is a phenomenon not well studied in bituminous binders. Note that the steric effects are inter- and intra-molecular (nonbonding) interactions dominated by steric repulsive forces, which manifest the shape and reactivity of interacting molecules. For instance, increasing the number and/or size of alkyl side groups attached to the carbon backbone, more steric hindrance is caused, leading to slower reaction rates.

The overall scope of this study was to examine the potential impact of the chemical composition of bituminous binders on the physical properties. Although previous studies investigated the relationships between the different chemical fractions and the rheology of bituminous binders, limited research was performed on elucidating the influence of the chemistry of fractions on the physical properties, such as glass transition and heat capacity, of binders of different grades. The next section presents the materials and characterisation methods employed to reach the objective of this study.

## Materials and methods

Two binders of classes 35/50 and 70/100 according to EN 12591, labelled Bitumen-1 and Bitumen-2, respectively, were used in this study. They came from the same refinery but with different paving grades. Conventional physical properties of these two binders, particularly the properties with penetration value at 25°C (for intermediate temperatures, EN 1426), softening point temperature (for high temperatures, EN 1427), and Fraass Breaking point temperature (for the low temperature cracking susceptibility, EN 12593) were measured and are reported in Table 1, indicating that Bitumen-1 was 'harder' than Bitumen-2. Performance Grade (PG) classes are also included in the table as used in North America for purchase specification, resulting from additional characterisation.

In addition to the conventional physical properties, characterisation was conducted using a Dynamic Shear Rheometer (DSR) and Bending Beam Rheometer (BBR) to address low, intermediate,

**Table 1.** Properties of studies binders.

| Sample | Penetration value at 25°C [×0.1-mm] | Softening point temperature [°C] | Frass breaking temperature [°C] | PG |
|---|---|---|---|---|
| Bitumen-1 | 39 | 54.4 | −12 | 70–22 |
| Bitumen-2 | 85 | 45.8 | −15 | 64–22 |

and high temperature behaviour. Firstly, DSR was run at a fixed frequency of 10 rad/s, in a temperature ramp of 6°C/min between −20 and 80°C, on a single testing geometry of 10-mm parallel plate and 2.5-mm gap height (Porot, 2019; Porot et al., 2020). The lower temperature tests were run in stress control, and the higher temperature was in strain control. While it may differ from other standardised testing methods, this experiment allows one to run the measurement in one single test and generate a continuous dataset, avoiding using shifting functions when building master curves (Porot, 2019). Moreover, BBR tests were employed to determine the low temperature properties (AASHTO M313). These tests were run on aged binders after RTFOT follow by PAV. Two different temperatures were used, −12 and −18°C for Bitumen-1 and −18 and −24°C for Bitumen-2, to match as close as possible the criteria for stiffness of 300 MPa and m-value of 0.3.

As mentioned earlier, bituminous binders are subdivided into two fractions: asphaltenes and maltenes. Based on the polarity, the latter can be further separated into saturates, aromatics, and resins. Recent studies have considered these fractions of maltene and asphaltenes to provide valuable insights into the chemical makeup of binders and the relationship between their fractions and mechanics (Eberhardsteiner et al., 2015; Hofko et al., 2016; Sakib et al., 2020; Sultana & Bhasin, 2014; Wang et al., 2021). In this research, a simple fractionation approach was adopted by emphasising exclusively asphaltenes and maltenes in assessing the chemistry and the thermal properties associated with the structural changes of binders. From both binders, the asphaltenes were obtained by precipitation in n-heptane, and the maltenes were recovered from the solvent afterward (ASTM D3279). The fractional composition of binders was respectively 15% asphaltenes and 85% maltenes for Bitumen-1 and 13% asphaltenes and 87% maltenes for Bitumen-2.

Fourier Transform Infrared (FTIR) spectroscopic analyses were performed in the samples in Attenuated Total Reflectance (ATR) mode to analyse the binders and their fractions chemically. The FTIR-ATR technique is powerful in characterising the chemical species of bituminous binder by identifying the various incorporated functional groups (Branthaver et al., 1993; Petersen, 1986). Proper model fitting also provides consistent and reliable information on specific fingerprints for bituminous binders (Porot et al., 2023). In this research, the measurement was run between 4000 and 600 $cm^{-1}$ with 64 scans and 4 $cm^{-1}$ resolution (Hofko et al., 2018; Mirwald et al., 2022). Note that asphaltenes used for chemical analyses in FTIR were in a solid state and stored in a sealed black tube in the dark. Applying a load on the asphaltene samples before running the measurement is needed to ensure sufficient contact surface on the crystal and obtain a stable signal for reliable results.

Finally, calorimetric analyses were performed on the binders and their fractions using a temperature modulated DSC (TM-DSC) to elucidate further the thermo-kinetics phenomena associated with the structural change of binders. The thermal properties of all samples were measured with a TM-DSC in a nitrogen flow of 50 mL/min. Firstly, the samples (6–10 mg) were heated at 165°C for 5 min. Afterward, they were cooled down at a rate of 2°C/min to −60°C, equilibrated at this temperature for 5 min and then heated to 300°C at 2°C/min, with 0.5°C temperature modulation of sawtooth mode every 60 s. This temperature modulation was based on a periodical step-scan signal superimposed on the linear temperature changes yielding a heating profile. All the $C_p$ calculations were performed using the StepScan function in Pyris software (PerkinElmer). The glass transition temperature ($T_g$) values were determined as the temperature at the half-height between the heat capacity of onset and endpoint of the glass transition region. With the TM-DSC, it is possible to separate kinetic processes and glass transitions by separating the overlapping reversing and non-reversing structural thermal processes upon temperature modulation of a heat flow. More details about TM-DSC and its importance in obtaining

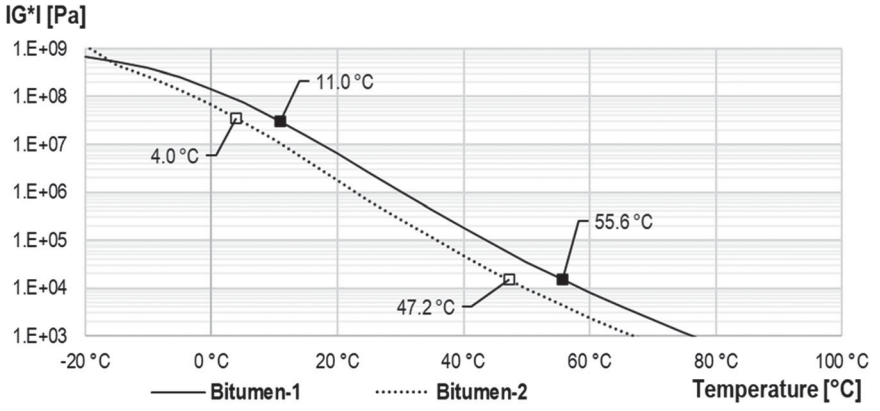


**Figure 1.** DSR shear stiffness modulus over temperature of studied binders.

accurate thermographs are provided in (Apostolidis et al., 2021). Three TM-DSC scans were performed for each binder and on asphaltenes and maltenes alone.

## Results and discussion

### *Rheological analyses of binders*

Figure 1 displays the shear modulus for binders as measured via DSR. The bold points were on the upper part for the cross-over parameters and the lower part for the equi-modulus at 15 kPa. The outcomes are consistent with the conventional physical properties, and Bitumen-1 was concluded to be 'harder' than Bitumen-2. The cross-over parameter, which indicates intermediate temperature, corresponds to the 45° phase angle as the transition between elastic to viscous predominant behaviour. The temperature at equi-modulus of 15 kPa is also foreseen as an indicator of high temperature, showing a relatively good correlation with softening point temperature for both neat and modified binders (Alisov et al., 2020; Radenberg & Gehrke, 2016). The difference between both binders was almost a parallel shift by about 8°C.

Figure 2 shows the BBR results for binders after RTFOT+PAV conditioning. In both cases, the critical temperature was driven by continuous stiffness temperature with a difference between stiffness and m-value temperatures of 1.6°C for Bitumen-1 and 1.9°C for Bitumen-2. The results are consistent with the Fraass Breaking Point temperature from Table 1, even though the latter was performed on original binders with no aging conditioning. The Bitumen-2 showed a lower BBR temperature.

### *Chemical compositional analyses of binders and fractions*

The scope of the chemical analyses using FTIR-ATR was to provide insight and understanding of functional groups in binders and their fractions by evaluating the infrared (IR) spectra. Firstly, FTIR was run on the binders to achieve this goal. Figure 3 displays the IR spectra for both binders. Only in the part where the significant spectra are shown, above 3100 $cm^{-1}$ and between 2700 and 1800 $cm^{-1}$, the spectra did not show significant peaks. The wavenumbers in the region greater than 3000 $cm^{-1}$ are assigned to aromatic C–H stretching, with the position of bands to be associated with the number of rings in aromatics. As expected, the highest absorption intensity was observed in the region between 2700 and 3100 $cm^{-1}$. Also, a different scale for absorption was used between 1800 and 600 $cm^{-1}$ to improve the visualisation of IR spectra differences. Both spectra almost perfectly overlapped at this point, and no significant difference can be noticed even if they displayed different rheological properties.

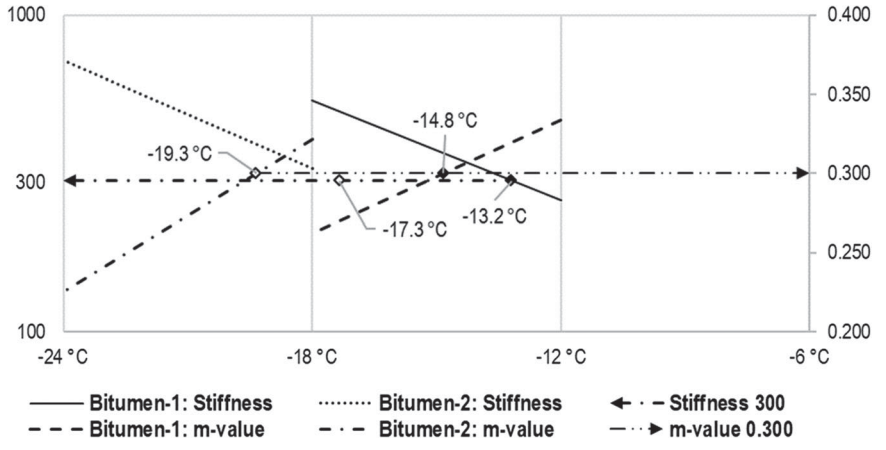


**Figure 2.** BBR results of studied binders.

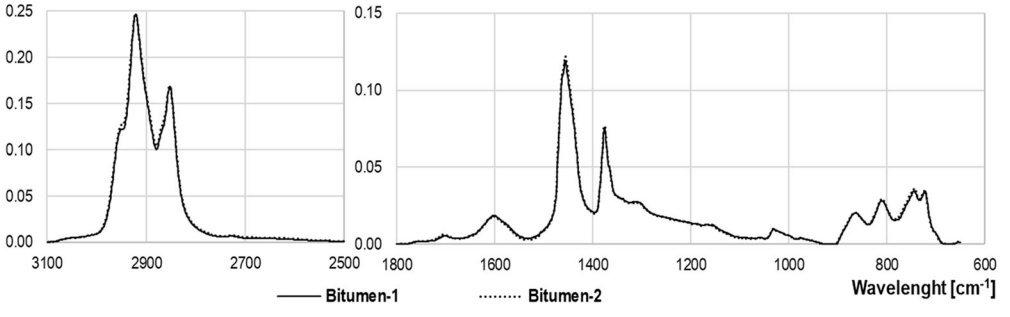


**Figure 3.** IR spectra of studied binders.

In a second step, analyses were performed on the bituminous fractions with precipitated asphaltenes and recovery maltenes. Figure 4 shows the comparison for Bitumen-1 between the binder and its fractions. All IR spectra displayed the same peaks but not necessarily the same absorption intensity. The asphaltene peaks were evenly spread along the spectra, while the maltenes still displayed higher peaks in the 2900 $cm^{-1}$ region. Also, the maltenes overlapped the binder in almost all bands, with the aliphatic groups (e.g. methyl, methylene, and methine) in the region between 3000 and 2750 $cm^{-1}$ being the far highest one. The bands at about 2920 and 2850 $cm^{-1}$ are assigned to the asymmetric stretching of methylene and the symmetric stretching of methylene, respectively. With the asphaltenes of Bitumen-1 (i.e. Asphaltene-1), the bands were more spread with generally lower absorption intensity for the aliphatic groups as compared to the binder. The low absorption level may also be biased because asphaltene is in solid powder form – it may result in air voids at the contact surface to the ATR unit. The same attribute was observed on Bitumen-2 and elsewhere (Lu et al., 2021).

Figure 5 compares the asphaltenes and maltenes from both binders separately. The IR spectra were almost superposed, although the appeared band near 1014 $cm^{-1}$ was sharper and more predominant for the asphaltenes of Bitumen-2 (i.e. Asphaltene-2). The 1014 $cm^{-1}$ band is attributed to C–H in-plane bending of aromatics and asymmetric C–O–C stretching of a mixture of (alkyl/aryl) ethers (Asemani & Rabbani, 2020) and is also associated with sulfoxide. In other words, Asphaltene-2 potentially contains aromatic rings attached to a mixture of ethers (alkyl and aryl) or sulfoxide. To this end, these compounds may be the reason for observing steric hindrance in Asphaltenes-2 in the next subsection. Note that the C–H in-plane bending bands of aromatics appear as several bands from weak

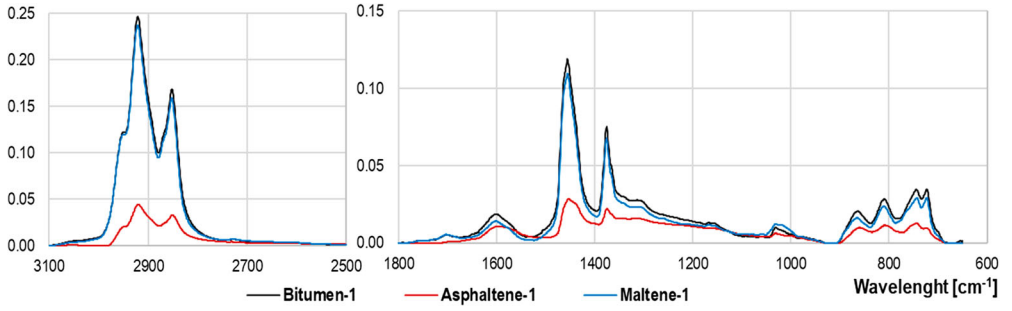


**Figure 4.** IR spectra of Bitumen-1 and its fractions.

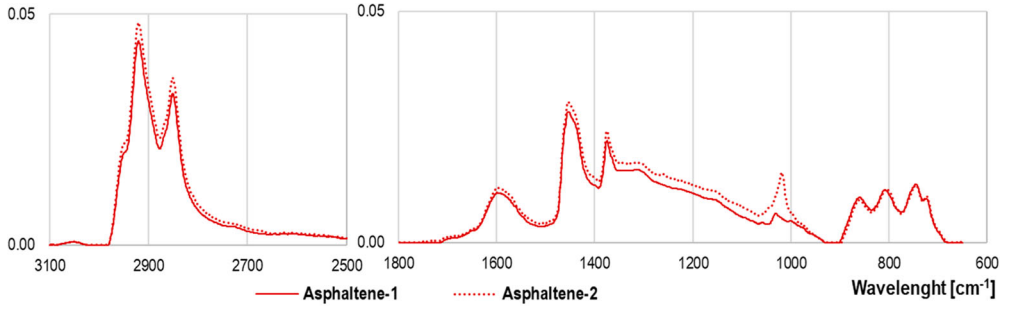


(a)

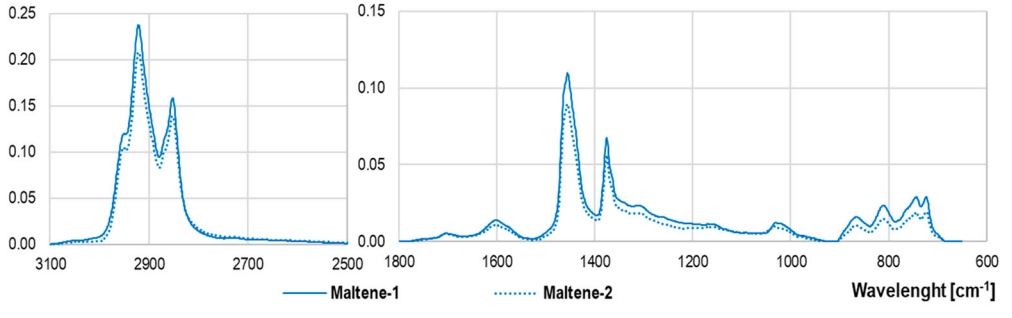


(b)

**Figure 5.** IR spectra of (a) asphaltenes and (b) maltenes from both binders.

to medium intensity in the region between 1200 and 800 $cm^{-1}$, and their position and intensity are associated with the pattern of the substitutions in aromatic rings (Smith, 1998).

## *Calorimetric analyses of binders and fractions*

The DSC thermograms over heating of two binders and their corresponding fractions are shown in Figures 6–8. Especially, as shown in Figure 7, for Bitumen-1, the binder and its maltenes showed similar calorimetric signals in the temperature range studied with the $T_g$ of maltenes (−18.0°C) to be lower than of the binder (−16.5°C), manifesting the ductile behaviour of maltenes comparing to the binders. The fact that binders consist of mixtures of maltenes and asphaltenes also reflects the impact of the

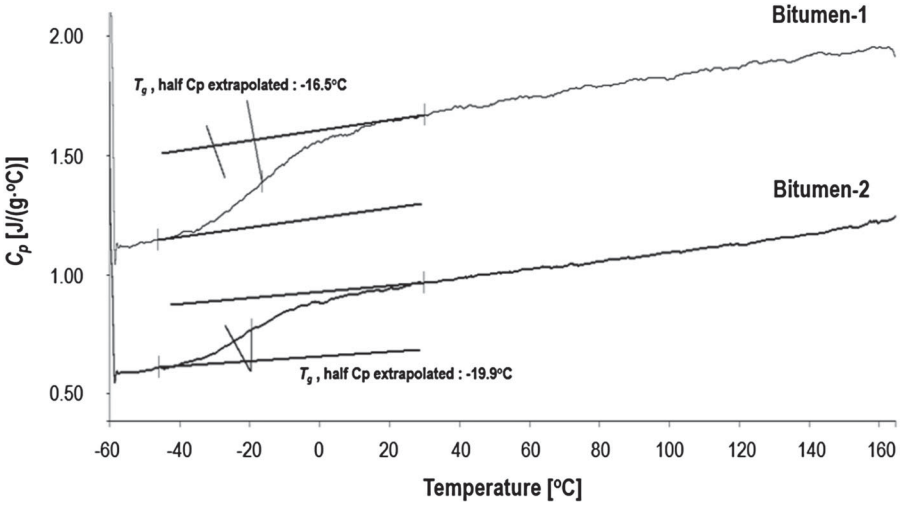


**Figure 6.** Heat capacity curves of studied binders over heating.

later fraction on the glass transition of binders. Nevertheless, no clear glass transition was seen in the heat capacity, $C_p$, curves of asphaltenes, as shown in Figures 7(b) and 8(b).

The $T_g$ values obtained from the $C_p$ curves of Bitumen-1 and its maltenes were higher than those of Bitumen-2 and its maltenes. This attribute is linked to the fact that Bitumen-2 was a 'softer' binder than Bitumen-1. In general, the $T_g$ can be used as an indication of the brittleness of bituminous binders. A binder with high $T_g$ is a brittle material prone to low-temperature thermal cracking and, thus, a high Fraass breaking point or BBR temperature. Thus, the maltenes are expected to show lower $T_g$ values than binders, as these fractions contain light hydrocarbons without heavy molecules, such as asphaltenes.

Important information about the structure of binders and their fractions is also provided by the $C_p$ change over the glass transition, $\Delta C_p$. The $C_p$ is defined as the amount of heat supplied to a material to produce a unit change in its temperature. On the one hand, the $\Delta C_p$ values of Bitumen-1 (0.24 J/(g·°C)) were identical to those of its maltenes (0.24 J/(g·°C)), indicating the limited influence of asphaltenes on the $\Delta C_p$. On the other hand, a significant difference in the $\Delta C_p$ values was observed between Bitumen-2 (0.29 J/(g·°C)) and its maltenes (0.35 J/(g·°C)) upon heating. Thus, it can be said that asphaltenes may play a role in structuring the Bitumen-2. Here, the glass transition attribute of asphalt bituminous binders is considered similar to the glass transition of an amorphous liquid. In this way, the structural state of binders could be reflected by their relative size of the repeat units. The size of these units can be estimated by calculating the ratio of $\Delta C_p$ of a mole of the mobile repeat unit of an amorphous liquid ($\Delta C_{p,ref}$), which is approximately 11 J/(mol·°C) (Wunderlich, 1960), to $\Delta C_p$ of the material of interest.

The relative size of mobile repeat units of Bitumen-2 and its maltenes was 37.8 and 31.8 g/mol, respectively, indicating the weight of constituent units, which are covalently linked or (nano)-aggregated in a solution. Interestingly, the size of units of Bitumen-1 (46.6 g/mol) and its maltenes (46.2 g/mol) was larger than that of Bitumen-2. It is believed that the large repeat units of Bitumen-1 could reflect that the latter ($T_g$: −16.5°C) was a stiffer and more brittle binder than Bitumen-2 ($T_g$: −19.9°C). Note that the values of the relative size of mobile repeat units cannot be considered as the average molecular weight of the material, such as 300–1000, 750, and 500 g/mol of bituminous binders, petroleum, and coal asphaltenes, respectively (Mullins, 2010).

The $T_g$ and $\Delta C_p$ values and the ratios of $\Delta C_p$s of all materials during heating and cooling are recorded in Table 2. The $T_g$ and $\Delta C_p$ values of both binders and their maltenes were higher in cooling

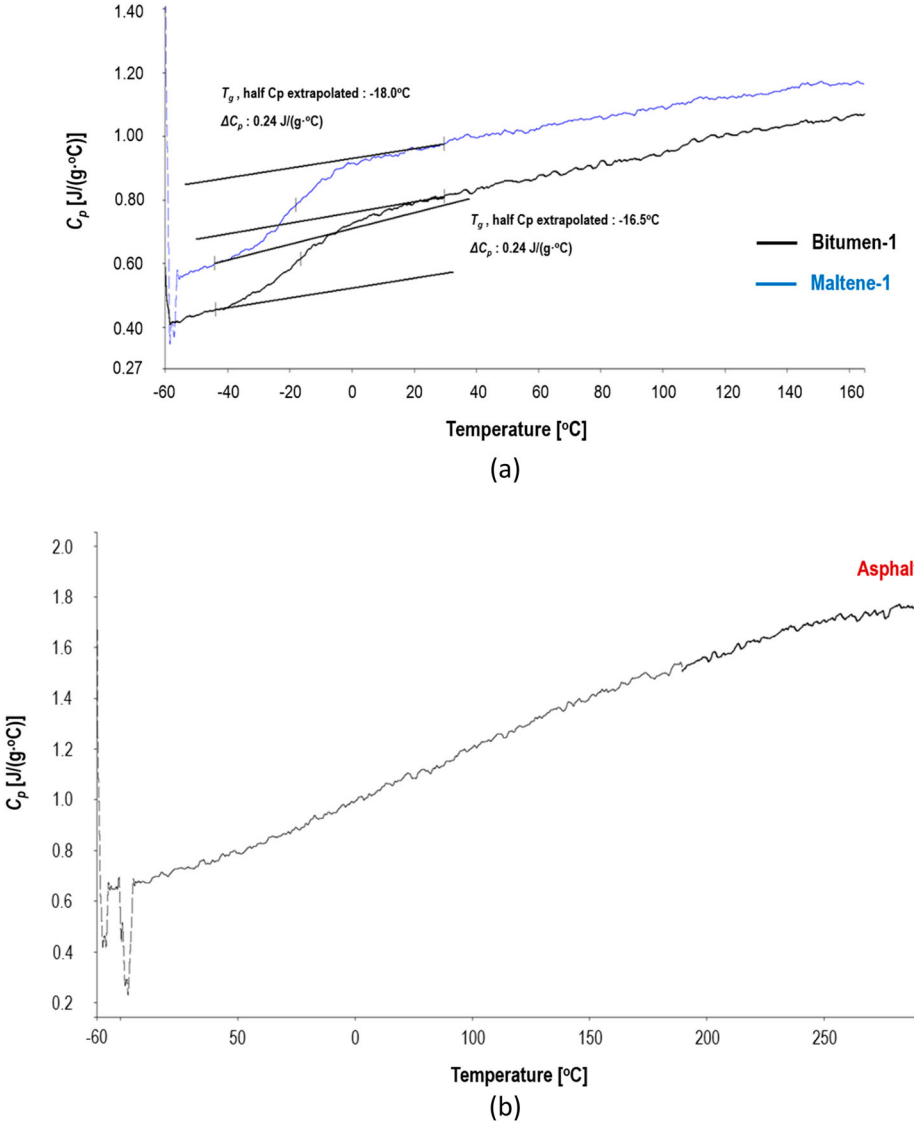


**Figure 7.** Heat capacity curves of (a) Bitumen-1 and Maltene-1, and (b) Asphaltene-1, over heating.

scans due primarily to thermal lag in the samples. Also, the glass transition of asphaltenes was hard to be revealed from the $C_p$ curves. Thus, further analyses of heat flow curves of the asphaltenes were conducted to elucidate the thermo-kinetics of these materials.

In Figure 9, a broad heat flow exotherm of Asphaltene-2 is revealed from 50 to 110°C, reflecting the steric hindrance of asphaltenes upon heating. For the 50–110°C range, the total exotherm, or heat flow released, in the heat flow curves of asphaltenes was −86.8 J/g upon heating and not apparent upon cooling, an attribute observed elsewhere as well (Chailleux et al., 2021; Ganeeva et al., 2014; Masson et al., 2005; Michon et al., 1999). The $T_g$ and $\Delta C_p$ values are given in Table 2.

The energy change events observed in the asphaltenes of Bitumen-2 (Asphaltene-2) in Figure 9 might be associated with the presence of aromatic rings attached to a mixture of ethers (alkyl and aryl) or sulfoxides, as observed from the chemical composition analyses in this research. In the case of the aromatic rings with ether content and alkyl side groups, a possible explanation is that the steric

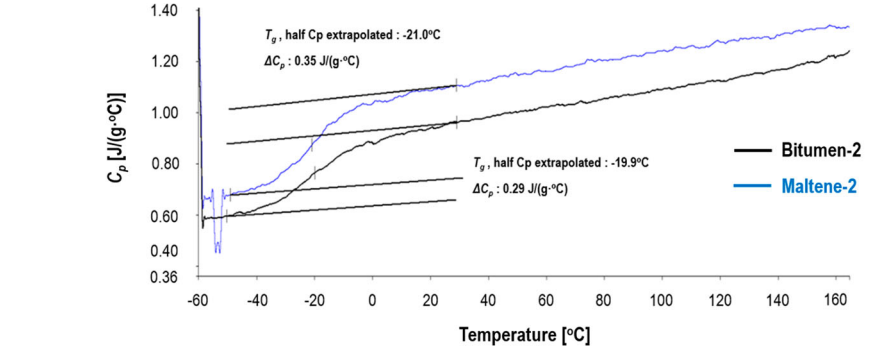


(a)

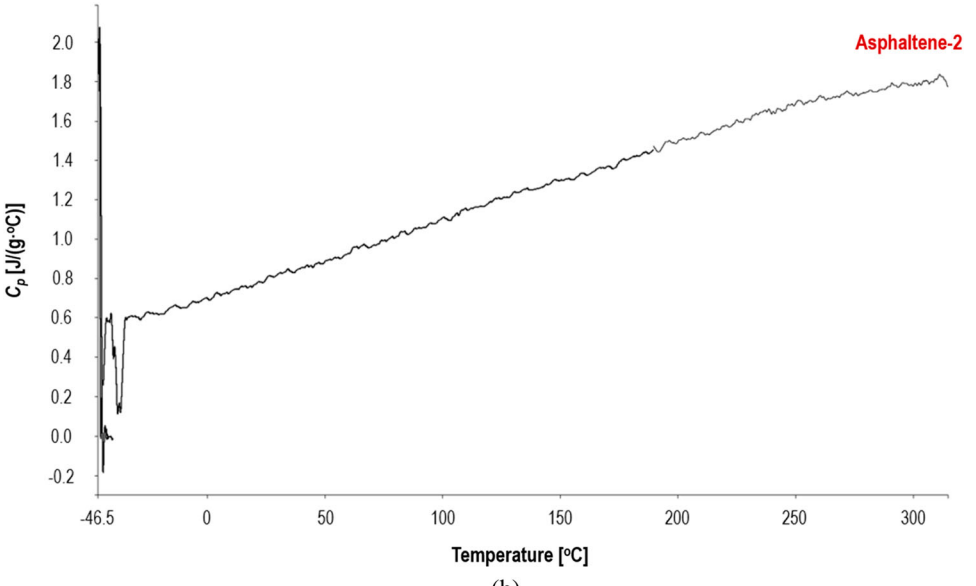


(b)

**Figure 8.** Heat capacity curves of (a) Bitumen-2 and Maltene-2, and (b) Asphaltene-2, over heating.

**Table 2.** Thermal properties of studied binders and their fractions.

| Sample | DSC run | $T_g$ [°C] | $\Delta C_p$ [J/(g·°C)] | $\Delta C_{p,ref}/\Delta C_p$ [g/mol] |
|---|---|---|---|---|
| Bitumen-1 | heating | −17.3 | 0.24 | 46.6 |
| | cooling | −16.0 | 0.38 | 28.9 |
| Maltene-1 | heating | −18.0 | 0.24 | 46.2 |
| | cooling | −16.4 | 0.39 | 28.3 |
| Asphaltene-1 | heating | | | |
| | cooling | | | |
| Bitumen-2 | heating | −22.0 | 0.29 | 37.8 |
| | cooling | −18.5 | 0.33 | 33.5 |
| Maltene-2 | heating | −21.0 | 0.35 | 31.8 |
| | cooling | −19.2 | 0.40 | 27.3 |
| Asphaltene-2 | heating | | | |
| | cooling | | | |

hindrance observed in Asphaltene-2 might occur due to the excessive intermolecular repulsive forces, preventing further aggregate growth. Considering the above, the large ether content containing alkyl side groups in Asphaltene-2 could reflect the large solubility of this fraction, which might have been

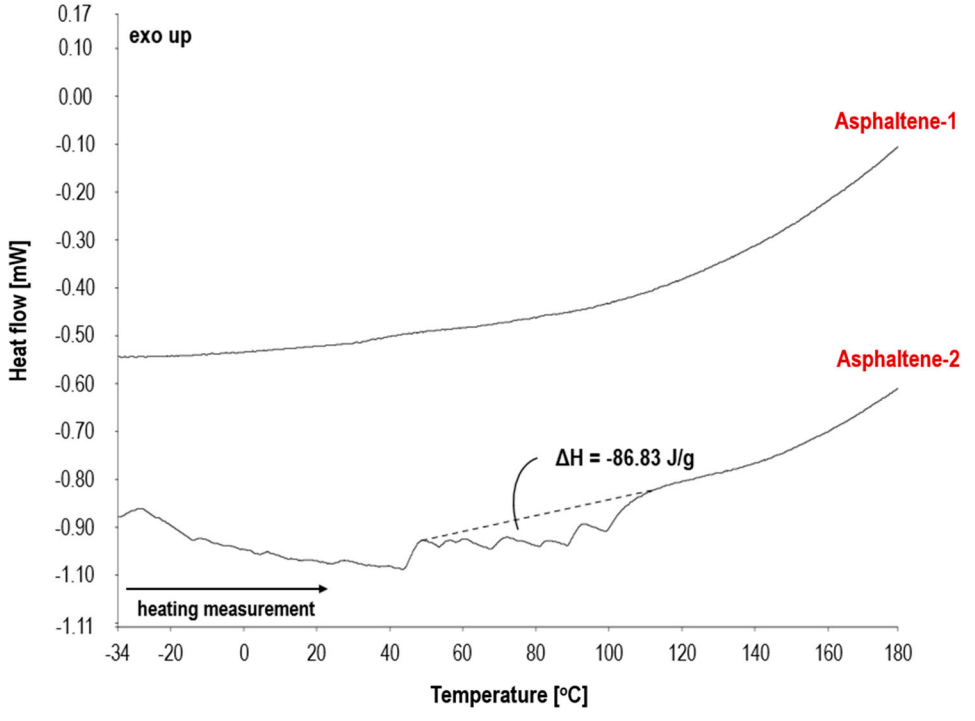


(a)

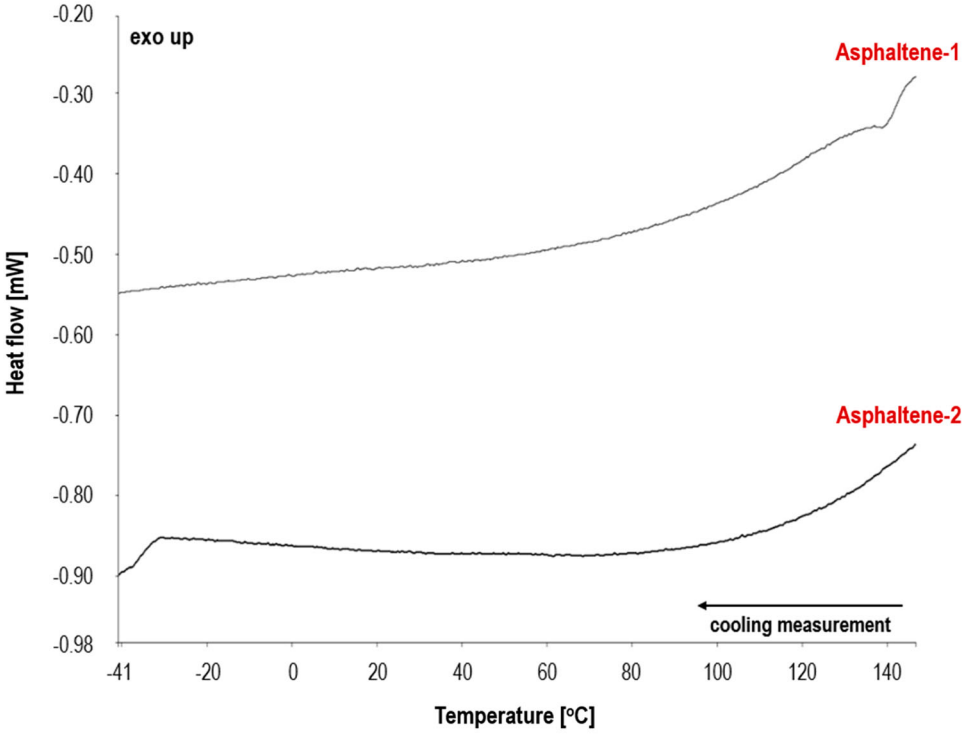


(b)

**Figure 9.** Heat flow curves of Asphaltene-1 and Asphaltene-2 upon (a) heating and (b) cooling.

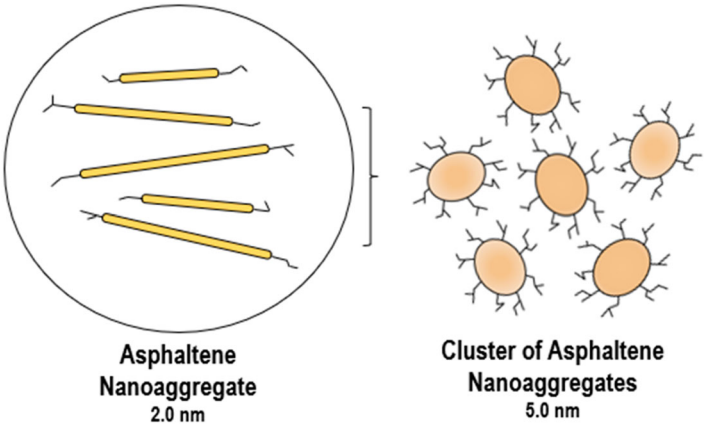


**Figure 10.** Yen-Mullins model demonstrating the dominant molecular architecture and colloidal structures for asphaltenes with peripheral alkanes.

the reason for selecting Bitumen-2 for polymer modification elsewhere (Apostolidis et al., 2021). Note that asphaltenes of low solubilities, like the large molecules of Asphaltene-1, have a more exposed aromatic core with fewer alkyl side groups and, subsequently less intermolecular attraction in the interior and steric repulsion on the periphery. This attribute is well explained by the Yen-Mullins model discussed in (Mullins, 2010; Mullins et al., 2012) and shown in Figure 10. Nevertheless, asphaltenes are still enigmatic substances and only by investigating their molecular structure and size it is possible to understand their origin and chemical/physical processes involved in the formation of nanoaggregate architectures.

## Conclusions

The objective of this research was to examine the differences in the physical properties of bituminous binders based on their chemical composition. Two binders from the same refinery but with different paving grades were selected in this research, and their asphaltene and maltene fractions were separated by precipitation. After conducting rheological analyses, the binders and their fractions were individually evaluated using Fourier transform infrared spectroscopy and differential scanning calorimetry.

Rheological results were consistent with the conventional physical measurements conducted on binders to address low to high temperature rheological behaviour. The binder with the higher content of asphaltenes has shown higher stiffness, BBR temperature, and glass transition temperature, suggesting that any difference in ratio between asphaltenes and maltenes could lead to differences in the binder behaviour.

From the chemical compositional analyses, it is challenging to correlate the physical properties of bituminous binders with their infrared spectra. Nevertheless, asphaltenes and maltenes displayed different spectra in band intensity, especially near 1014 $cm^{-1}$. This attribute dictates that the asphaltenes of the soft binder might be rich in large-fused aromatic rings with significant alkyl carbon content or sulfoxide. This observation is supported by calorimetric measurements where steric hindrance occurred in the same asphaltenes upon heating.

Comparison of heat capacity and heat flow curves of binders and their fractions have shown that, on the one hand, maltenes contribute significantly to the overall glass transition behaviour of binders as they form the medium where asphaltenes are dispersed. The asphaltenes considerably also affect the steric hindrance, but the extent of influence is highly related to the solubility of asphaltenes. Note that the impact of asphaltenes on the heat capacity changes in glass transition was limited.

While this research investigated the contribution of asphaltenes and maltenes to the physical properties of bituminous binders, further work is needed to examine the differences in the chemistry of binders from different refineries. The present findings from this research could be used as a first step to establish a new analytical approach for bituminous binders toward understanding the physical properties difference of binders based on their chemical composition.

## Disclosure statement

No potential conflict of interest was reported by the author(s).

## ORCID

*Laurent Porot* http://orcid.org/0000-0002-7173-9035
*Panos Apostolidis* http://orcid.org/0000-0001-5635-4391

## References

Adams, J. J., Elwardany, M. D., Planche, J. P., Boysen, R. B., & Rovani, J. F. (2019). Diagnostic techniques for various asphalt refining and modification methods. *Energy & Fuels*, *33*(4), 2680–2698. https://doi.org/10.1021/acs.energyfuels.8b03738

Alisov, A., Riccardi, C., Schrader, J., Falchetto, A. C., & Wistuba, M. P. (2020). A novel method to characterise asphalt binder at high temperature. *Road Materials and Pavement Design*, *21*(1), 143–155. https://doi.org/10.1080/14680629.2018.1483258

Apostolidis, P., Elwardany, M. D., Porot, L., Vansteenkiste, S., & Chailleux, E. (2021). Glass transitions in bituminous binders. *Materials and Structures*, *54*(3), 132. https://doi.org/10.1617/s11527-021-01726-6

Asemani, M., & Rabbani, A. R. (2020). Detailed FTIR spectroscopy characterization of crude oil extracted asphaltenes: Curve resolve of overlapping bands. *Journal of Petroleum Science and Engineering*, *185*, 106618. https://doi.org/10.1016/j.petrol.2019.106618

Branthaver, J., Petersen, J. C., Robertson, R. E., Duvall, J. J., Kim, S. S., Harnsberger, P. M., Mill, T., Barbour, E. K., Ensley, E. K., Barbour, F. A., & Scharbron, J. F. (1993). *Binder characterization and evaluation. Volume 2: Chemistry*. (Report No. SHRP-A-368). Strategic Highway Research Program.

Chailleux, E., Queffélec, C., Borghol, I., Farcas, F., Marceau, S., & Bujoli, B. (2021). Bitumen fractionation: Contribution of the individual fractions to the mechanical behavior of road binders. *Construction and Building Materials*, *271*, 121528. https://doi.org/10.1016/j.conbuildmat.2020.121528

Corbett, L. W. (1969). Composition of asphalt based on generic fractionation, using solvent deasphaltening, elution-adsorption chromatography, and densimetric characterization. *Analytical Chemistry*, *41*(4), 576–579. https://doi.org/10.1021/ac60273a004

Eberhardsteiner, L., Füssl, J., Hofko, B., Handle, F., Hospodka, M., Blab, R., & Grothe, H. (2015). Influence of asphaltene content on mechanical Bitumen behavior: Experimental investigation and micromechanical modeling. *Materials and Structures*, *48*(10), 3099–3112. https://doi.org/10.1617/s11527-014-0383-7

Evdokimov, I. N., & Losev, A. P. (2010). Electrical conductivity and dielectric properties of solid asphaltenes. *Energy & Fuels*, *24*(7), 3959–3969. https://doi.org/10.1021/ef1001887

Ganeeva, Y. M., Yusupova, T. N., Romanov, G. V., & Bashkirtseva, N. Y. (2014). Phase composition of asphaltenes. *Journal of Thermal Analysis and Calorimetry*, *115*(2), 1593–1600. https://doi.org/10.1007/s10973-013-3442-3

Hofko, B., Eberhardsteiner, L., Füssl, J., Grothe, H., Handle, F., Hospodka, M., Grossegger, D., Nahar, S. N., Schmets, A. J. M., & Scarpas, A. (2016). Impact of maltene and asphaltene fraction on mechanical behavior and microstructure of Bitumen. *Materials and Structures*, *49*(3), 829–841. https://doi.org/10.1617/s11527-015-0541-6

Hofko, B., Porot, L., Falchetto Cannone, A., Poulikakos, L., Huber, L., Lu, X., Mollenhauer, K., & Grothe, H. (2018). FTIR spectral analysis of bituminous binders: Reproducibility and impact of ageing temperature. *Materials and Structures*, *51*(2), 45. https://doi.org/10.1617/s11527-018-1170-7

Hunter, R., Self, A., & Read, J. (2015). *The shell Bitumen handbook* (6th ed.). Default Book Series.

Kamkar, M., & Natale, G. (2021). A review on novel applications of asphaltenes: A valuable waste. *Fuel*, *285*, 119272. https://doi.org/10.1016/j.fuel.2020.119272

Kopsch, H. (1994). On the thermal behavior of petroleum asphaltenes. *Thermochimica Acta*, *235*(2), 271–275. https://doi.org/10.1016/0040-6031(94)85171-9

Lesueur, D. (2009). The colloidal structure of Bitumen: Consequences on the rheology and on the mechanisms of Bitumen modification. *Advances in Colloid and Interface Science*, *145*(1-2), 42–82. https://doi.org/10.1016/j.cis.2008.08.011

Lu, X., Soenen, H., Sjövall, P., & Pipintakos, G. (2021). Analysis of asphaltenes and maltenes before and after long-term aging of Bitumen. *Fuel*, *304*, 121426. https://doi.org/10.1016/j.fuel.2021.121426

Masson, J.-F., Collins, P., & Polomark, G. (2005). Steric hardening and the ordering of asphaltenes in Bitumen. *Energy & Fuels*, *19*(1), 120–122. https://doi.org/10.1021/ef0498667

Masson, J. F., Polomark, G. M., & Collins, P. (2002). Time-Dependent microstructure of Bitumen and its fractions by modulated differential scanning calorimetry. *Energy & Fuels*, *16*(2), 470–476. https://doi.org/10.1021/ef010233r

Michon, L. C., Netzel, D. A., Turner, T. F., Martin, D., & Planche, J. P. (1999). A $^{13}$C NMR and DSC study of the amorphous and crystalline phases in asphalts. *Energy & Fuels*, *13*(3), 602–610. https://doi.org/10.1021/ef980184r

Mirwald, J., Nura, D., & Hofko, B. (2022). Recommendations for handling Bitumen prior to FTIR spectroscopy. *Materials and Structures*, *55*(2), 26. https://doi.org/10.1617/s11527-022-01884-1

Mullins, O. C. (2010). The modified Yen model. *Energy & Fuels*, *24*(4), 2179–2207. https://doi.org/10.1021/ef900975e

Mullins, O. C., Sabbah, H., Eyssautier, J., Pomerantz, A. E., Barré, L., Andrews, A. B., Ruiz-Morales, Y., Mostowfi, F., McFarlane, R., Goual, L., Lepkowicz, R., Cooper, T., Orbulescu, J., Leblanc, R. M., Edwards, J., & Zare, R. N. (2012). Advances in asphaltene science and the Yen-Mullins model. *Energy & Fuels*, *26*(7), 3986–4003. https://doi.org/10.1021/ef300185p

National Academies of Sciences, Engineering and Medicine. (2017). *Relationship between chemical makeup of binders and engineering performance*. National Academy of Sciences. https://doi.org/10.17226/24850

Petersen, C. (1986). Quantitative functional group analysis of asphalts using differential infrared spectrometry and selective chemical reactions - Theory and application. *Transportation Research Record*, *1096*, 1–11.

Porot, L. (2019). *Rheology and bituminous binder. A review of different analyses*. RILEM 252-CMB Symposium 2018 RILEM Bookseries 20. https://doi.org/10.1007/978-3-030-00476-7_9

Porot, L., Büchner, J., Steinder, M., Damen, S., Hofko, B., & Wistuba, M. P. (2020). *Comparison of different DSR protocols to characterise asphalt binders*. ISBM RILEM symposium Lyon 2020, RILEM Bookseries. https://doi.org/10.1007/978-3-030-46455-4

Porot, L., Mouillet, V., Margaritis, A., Haghshenas, H., Elwardany, M., & Apostolidis, P. (2023). Fourier-Transform infrared analysis and interpretation for Bituminous binders. *Road Materials and Pavement Design*, *24*(2), 462–483. https://doi.org/10.1080/14680629.2021.2020681

Radenberg, M., & Gehrke, M. (2016). *Assessing Bitumen in the whole service-temperature-range with the dynamic shear rheometer*. In 6th Eurasphalt & Eurobitume Congress, Prague, Czech Republic.

Sakib, N., Hajj, R., Hure, R., Alomari, A., & Bhasin, A. (2020). Examining the relationship between Bitumen polar fractions, rheological performance benchmarks, and tensile strength. *Journal of Materials in Civil Engineering*, *32*(6), 04020143. https://doi.org/10.1061/(ASCE)MT.1943-5533.0003197

Schuler, B., Zhang, Y., Liu, F., Pomerantz, A. E., Andrews, A. B., Gross, L., Pauchard, V., Banerjee, S., & Mullins, O. C. (2020). Overview of asphaltene nanostructures and thermodynamic applications. *Energy & Fuels*, *34*(12), 15082–15105. https://doi.org/10.1021/acs.energyfuels.0c00874

Smith, B. C. (1998). *Infrared spectral interpretation: A systematic approach*. CRC Press.

Sultana, S., & Bhasin, A. (2014). Effect of chemical composition on rheology and mechanical properties of asphalt binder. *Construction and Building Materials*, *72*, 293–300. https://doi.org/10.1016/j.conbuildmat.2014.09.022

Wang, Y., Zhao, K., Li, F., Gao, Q., & Lai, K. W. C. (2021). Asphaltenes in asphalt: Direct observation and evaluation of their impacts on asphalt properties. *Construction and Building Materials*, *271*, 121862. https://doi.org/10.1016/j.conbuildmat.2020.121862

Wunderlich, B. (1960). Study of the change in specific heat of monomeric and polymeric glasses during the glass transition. *The Journal of Physical Chemistry*, *64*(8), 1052–1056. https://doi.org/10.1021/j100837a022

Yasar, M., Akmaz, S., & Gurkaynak, M. A. (2007). Investigation of glass transition temperatures of turkish asphaltenes. *Fuel*, *86*(12-13), 1737–1748. https://doi.org/10.1016/j.fuel.2006.12.022

Zhang, Y., Takanohashi, T., Sato, S., Saito, I., & Tanaka, R. (2004). Observation of glass transition in asphaltenes. *Energy & Fuels*, *18*(1), 283–284. https://doi.org/10.1021/ef0301147